



Alleviation of heavy metal and silver nanoparticle toxicity and enhancement of their removal by hydrogen sulfide in *Phanerochaete chrysosporium*



Zhenzhen Huang^{a,1}, Kai He^{a,1}, Zhongxian Song^{b,1}, Guangming Zeng^{a,*}, Anwei Chen^{c,**}, Lei Yuan^a, Hui Li^a, Guiqiu Chen^a

^a College of Environmental Science and Engineering, Hunan University and Key Laboratory of Environmental Biology and Pollution Control (Hunan University), Ministry of Education, Changsha 410082, PR China

^b School of Municipal and Environmental Engineering, Henan University of Urban Construction, Pingdingshan 467036, PR China

^c College of Resources and Environment, Hunan Agricultural University, Changsha 410128, PR China

HIGHLIGHTS

- H₂S can greatly improve the removal of metal ions and total Ag from wastewater.
- A dose-dependent increase in cell survival was evoked by H₂S under toxicant stress.
- Application of H₂S significantly enhanced the expression of SOD and CAT activities.
- MDA and O₂⁻ levels were alleviated in *P. chrysosporium* cells pretreated with H₂S.
- Inhibition in oxidative stress was ascribed to upregulation in antioxidant enzymes.

ARTICLE INFO

Article history:

Received 19 November 2018

Received in revised form

19 February 2019

Accepted 27 February 2019

Available online 28 February 2019

Handling Editor: Tamara S. Galloway

Keywords:

Hydrogen sulfide

Heavy metals

Silver nanoparticles

Bioremediation

Antioxidant response

Phanerochaete chrysosporium

ABSTRACT

Hydrogen sulfide (H₂S), an important cellular signaling molecule, plays vital roles in mediating responses to biotic/abiotic stresses. Influences of H₂S on metal removal, cell viability, and antioxidant response of *Phanerochaete chrysosporium* upon exposure to heavy metals and silver nanoparticles (AgNPs) in the present study were investigated. An enhancement in Pb(II) removal with an increase in concentration of the H₂S donor sodium hydrosulfide (NaHS) was observed, and the maximum removal efficiencies increased by 31% and 17% under 100 and 200 mg/L Pb(II) exposure, respectively, in the presence of 500 μM NaHS. Application of 500 μM NaHS increased the cell viability by 15%–39% under Pb(II) stress (10–200 mg/L) with relative to the untreated control. Increase in total Ag uptake and cell survival was also elicited by NaHS in a concentration-dependent manner under AgNP stress. Meanwhile, activities of superoxide dismutase and catalase were significantly enhanced with the introduction of NaHS under stresses of Pb(II), Cd(II), Cu(II), Zn(II), Ni(II), and AgNPs. The inhibition in lipid peroxidation and oxidative stress was observed in *P. chrysosporium* cells exposed to these toxicants following NaHS pretreatment, which could be attributed to the upregulation in antioxidant enzymes. The results obtained suggest that H₂S can alleviate heavy metals and AgNP-induced toxicity to *P. chrysosporium* and improve the removal efficiency of these toxicants from wastewater.

© 2019 Elsevier Ltd. All rights reserved.

* Corresponding author.

** Corresponding author.

E-mail addresses: zgming@hnu.edu.cn (G. Zeng), A.Chen@hunau.edu.cn (A. Chen).

¹ These authors contribute equally to this article.

1. Introduction

Heavy metal contamination in water and soil has been one of the most concerned global environmental problems due to the increasing anthropogenic and industrial activities (Fang et al., 2016; Tang et al., 2018; Ye et al., 2017a,b; Zhang et al., 2019). Excess exposure to heavy metals results in the deterioration of

environmental quality and causes serious effects on the development of microorganisms, plants, animals, and humans because of their long-term toxic effects, carcinogenicity, and mutagenicity (Houda et al., 2016; He et al., 2018a,b,c; Ren et al., 2018a,b; Wang et al., 2018). It is reported that lead (Pb), cadmium (Cd), chromium (Cr), copper (Cu), nickel (Ni), and zinc (Zn) are the major heavy metal toxicants (Macomber and Hausinger, 2011; Ye et al., 2017a,b; Qin et al., 2018; Zhou et al., 2018; Wang et al., 2013). Trace amounts of these toxicants are able to cause colonization inhibition, membrane damage, oxidative stress, antioxidant enzyme upregulation, chromosome aberration, and even cell death (Gong et al., 2009; Huang et al., 2015; Ali et al., 2014). In addition, explosion in the use of silver nanoparticles (AgNPs), such as antimicrobial and sterile applications, also possesses environmental risks to human health and ecosystem (Choi et al., 2018; He et al., 2017a, 2018a and b). Both AgNPs themselves and released Ag^+ can induce generation of reactive oxygen species (ROS) and cytotoxicity through direct damage to cell membrane of some aquatic organisms and microbes in biological wastewater treatment processes (Wu et al., 2017; Zhang et al., 2018; Yang et al., 2018a,b). Meanwhile, it has been documented that Ag speciation and precipitation are potentially changed due to alteration in transport and fate of AgNPs under environmental stress, thus influencing their toxicity against aquatic organisms (McGillicuddy et al., 2017; Yi et al., 2018; Yang et al., 2018a,b; Xiong et al., 2018; Leng et al., 2019).

Bioremediation is an economic, efficient, and environmentally friendly alternative for removal of heavy metals (He et al., 2017b; Mir-Tutusaus et al., 2018). *Phanerochaete chrysosporium*, a typical species of white rot fungi, has been proven to be available for the treatment of wastewater containing heavy metals and AgNPs due to its admirable biosorption capacity (Xu et al., 2012a and b). However, the efficiency of *P. chrysosporium* in removal of heavy metals and AgNPs is still limited due to its lower resistance to toxic pollutants and longer bioremediation time. Hydrogen sulfide (H_2S) has been used to assist in 2,4-dichlorophenol (2,4-DCP) biodegradation by *P. chrysosporium* in our previous study (Chen et al., 2014). Therefore, it is worth further exploring whether this exogenous material can improve bioremediation capability of heavy metals and AgNPs.

H_2S , a new gaseous signal molecule, has been recommended for mediating a variety of physiological processes and defense responses against to biotic and abiotic stresses including heavy metals (Chen et al., 2018). More recent evidences have indicated that H_2S can exert antiinflammatory, antioxidant, antiapoptotic, cytoprotective, and organ-protective effects, further improving environmental stress tolerance of cells (Yuan et al., 2017). The protective roles of H_2S in plants could be attributed to the decreased influx and transport of metals and the elevated antioxidant enzymatic systems, including superoxide dismutase (SOD), catalase (CAT), peroxidase, and non-enzymatic constituents (He et al., 2018a,b,c). Enhancement in enzyme activities, such as SOD, CAT, and reduced glutathione, leads to the decreases in malonyldialdehyde (MDA) content and ROS production. In addition to the improvement of antioxidant enzymes, H_2S , as a reductive substance, can also scavenge ROS directly, such as superoxide (O_2^-) and hydrogen peroxide (Geng et al., 2004; Mitsuhashi et al., 2006). However, little information is available on the introduction of H_2S to bioremediation using microorganisms, especially fungi. Moreover, whether H_2S can alleviate the toxic effects induced by heavy metals and nanomaterials, and improve the biological treatment efficiency remains an open question. Thus, the aim of this study was to investigate the effects of H_2S on the bioremediation efficiency, cell viability, oxidative damage, and antioxidant enzyme activities of *P. chrysosporium* under stresses of Pb(II), Cd(II), Cu(II), Ni(II), Zn(II), and AgNPs. *P. chrysosporium* was pretreated with the H_2S donor

sodium hydrosulfide (NaHS) prior to exposure to these toxicants.

2. Materials and methods

2.1. Strain culture

P. chrysosporium strain BKMF-1767 (CCTCC AF96007) obtained from the China Center for Type Culture Collection (Wuhan, China) was maintained on malt extract agar slants at 4 °C. Spore suspensions were prepared by gently scraping the spores from the agar surface into sterile ultrapure water and blending them evenly. The fungal spore suspensions at a concentration of 2.0×10^6 CFU/mL were inoculated into the culture medium and cultivated at 37 °C under 150 rpm. After 3 days of incubation, *P. chrysosporium* mycelia were harvested and rinsed several times for further use.

2.2. Characterizations of AgNPs

Polyethylene glycol-coated AgNPs (PVP-AgNPs) used in this work were obtained from NanoAmor (Houston, TX). The PVP-AgNP powders were suspended in ultrapure water, mixed with ultrasonic agitation, and stored at 4 °C in dark for further use. The as-prepared AgNPs were monodispersed and spherical in shape with an average particle diameter of 57.3 ± 15.5 nm on the basis of transmission electron microscopy (TEM) observations (Fig. 1). The mean

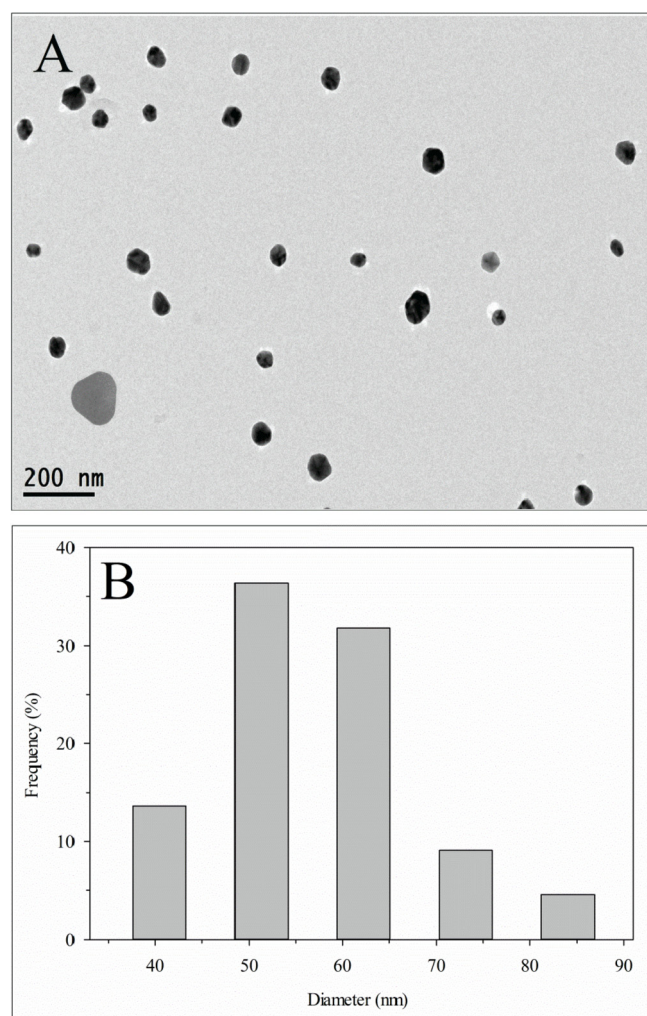


Fig. 1. AgNP characterizations: (A) representative TEM micrograph; (B) histogram of particle size distribution obtained from corresponding TEM images.

hydrodynamic diameter of AgNPs was also determined with the value of 85.1 ± 2.7 nm by dynamic light scattering (DLS) with a Zetasizer Nano-ZS (Malvern Instrument, U.K.). Difference in size distributions obtained from TEM and DLS methods arises from their different measurement principles (Huang et al., 2017). Besides, the zeta-potential of AgNPs showed a negative value of -10.8 ± 0.8 mV, and the dissolved fractions of AgNP stock suspensions were found to be less than 1% by monitoring the filtrates after ultrafiltration centrifugation using ICP-MS. After digestion of the samples using HNO_3 and H_2O_2 , total Ag concentration in aqueous solutions was determined by a flame atomic absorption spectroscopy (FAAS, PerkinElmer AA700, USA) (Huang et al., 2018a,b).

2.3. Effect of H_2S on removal of heavy metals and AgNPs

The influences of different concentrations of H_2S on Pb(II) and total Ag removal were investigated. After pretreatment with NaHS (0, 50, 100, and 500 μM) for 4 h, *P. chrysosporium* pellets were transferred to aqueous solutions containing 10, 50, 100, and 200 mg/L Pb(II) and AgNPs separately for another 78 h. Furthermore, a comparative experiment on removal of various heavy metals was also performed. The fungal pellets were pretreated with 100 μM NaHS for 4 h and then exposed to 100 mg/L Cd (II), Cu(II), Ni(II), and Zn (II), separately. Cultures that were treated with 0–500 μM NaHS but without heavy metals or AgNPs were used as controls. The culture media were taken at predetermined intervals for analysis of residual heavy metal concentrations. Concentrations of heavy metals in the aqueous solutions were monitored by using FAAS.

2.4. Physiological assays

After pretreatment with NaHS (0–100 μM), *P. chrysosporium* pellets, that were exposed to Pb(II), Cd (II), Cu(II), Ni(II), Zn (II), and AgNPs at initial concentrations of 100 mg/L for 24 h, were harvested and washed three times with ultrapure water for physiological analyses, including cell viability, lipid peroxidation, O_2^- generation, and antioxidant enzymes. For cell viability assays, prolonged exposure (78 h) to 10–200 mg/L Pb(II) and AgNPs with and without NaHS pretreatments was also carried out. Cell viability was assessed by MTT method according to Chen et al. (2014).

The content of malondialdehyde (MDA), a cytotoxic product of lipid peroxidation, was measured following our previous procedures (Zeng et al., 2012; Huang et al., 2018c). O_2^- generation was detected according to Chen et al. (2014) with minor modifications. Briefly, fungal samples (0.2 g) were homogenized in 2.5 mL of phosphate buffer (50 mM, pH 7.8). 1 mL of the extracts was added into 0.9 mL of 50 mM phosphate buffer and 0.1 mL of 10 mM hydroxylamine hydrochloride. After 20 min of reaction at 25 °C, 1 mL of 17 mM *p*-aminobenzenesulfonic acid and 1 mL of 7 mM *a*-naphthylamine were introduced into the mixture, which was incubated at 25 °C for another 20 min. Absorbance of the mixture was recorded at 530 nm by spectrophotometry. *P. chrysosporium* viability and O_2^- levels were expressed as relative percentages to the untreated control.

The activities of antioxidant enzymes SOD and CAT were measured following the method described by Zeng et al. (2012) and Huang et al. (2018a,b,c). SOD activity was detected by monitoring 50% inhibition of nitroblue tetrazolium chloride reduction. CAT activity was tested by monitoring the absorbance of H_2O_2 at 240 nm and one unit of CAT was defined as a decrease of 0.1 unit of A_{240} per min.

All assays were conducted in triplicate. The data were statistically analyzed by SPSS 22.0 software and expressed as the means \pm standard deviations. Statistical differences between the

experimental groups were determined using one-way analysis of variance, followed by Tukey post-hoc test. Differences of $p < 0.05$ were considered to be statistically significant.

3. Results and discussion

3.1. Promoting effects of H_2S on Pb(II) removal

Effects of H_2S on Pb(II) removal by *P. chrysosporium* were investigated under stress of 10–200 mg/L Pb(II). As shown in Fig. 2A–D, no obvious changes in Pb(II) removal are observed for low-concentration NaHS pretreatments (0–100 μM). Further increase in NaHS concentration (up to 500 μM) results in a significant promotion in Pb(II) removal efficiency. Although the maximum removal efficiencies for NaHS (0–500 μM) pretreatments all arrived at 100% at the initial Pb(II) concentration of 10 and 50 mg/L, 500- μM NaHS pretreatment elicited higher Pb(II) removal efficiency for short-term exposure (1–24 h) (Fig. 2A and B). The removal efficiencies under 100 and 200 mg/L Pb(II) treatments were also markedly increased by higher-dose NaHS during the whole adsorption process, with an increase of 31% and 17%, respectively, in the maximum removal efficiency of Pb(II) relative to the samples without NaHS (Fig. 2C and D). These findings indicated that Pb(II) removal by *P. chrysosporium* was enhanced after NaHS pretreatment, especially at higher concentrations, and the time to achieve higher removal efficiencies was shortened greatly. Similar results were reported for promotion of 2,4-DCP degradation by 50–100 μM NaHS (Chen et al., 2014). Besides, our previous studies found that the pH levels increased with increasing reaction time (Huang et al., 2015, 2017). Thus, another possibility for higher Pb(II) removal could be the formation of the precipitation of Pb(II) ions.

3.2. Effects of H_2S on total Ag removal

A promoting effect of H_2S was also observed on total Ag removal at NaHS concentration of 50 μM . The maximum percentages of total Ag removal were 56%, 68%, 90%, and 70.0% at the AgNPs concentration of 10, 50, 100, and 200 mg/L, respectively (Fig. 3). It was found that higher Ag removal efficiencies were obtained at moderate concentrations of AgNPs. In addition, it was also observed that exposure to 200 mg/L AgNPs showed higher removal efficiency of total Ag under 100- μM NaHS pretreatment. However,

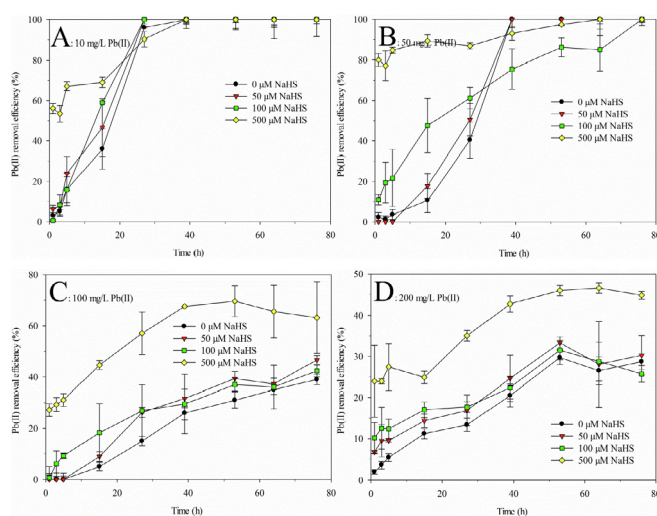


Fig. 2. Effects of different concentrations of H_2S on Pb(II) removal by *P. chrysosporium* after exposure to (A) 10, (B) 50, (C) 100, and (D) 200 mg/L Pb(II).

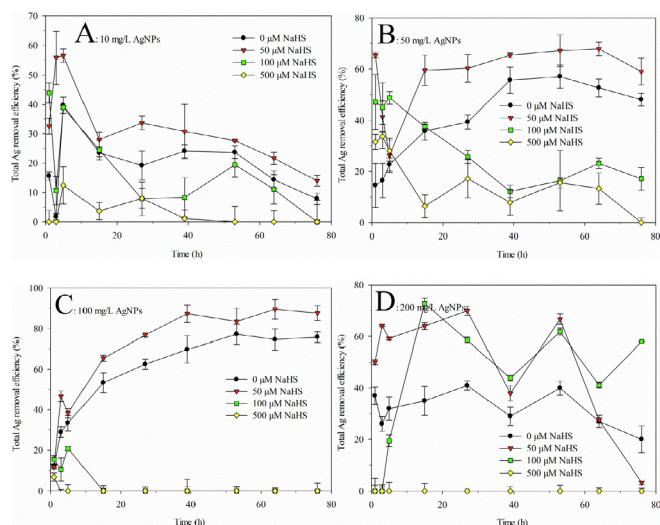


Fig. 3. Effects of different concentrations of H_2S on total Ag removal by *P. chrysosporium* under stresses of (A) 10, (B) 50, (C) 100, and (D) 200 mg/L AgNPs.

pretreatments with higher NaHS concentrations (500 μM) induced a clear dose-dependent efficiency reduction in total Ag removal, reaching undetectable levels in all AgNP-treated groups. The findings indicated that Ag uptake by *P. chrysosporium* mycelium could be closely related to the concentrations of NaHS and AgNPs. AgNPs with higher initial concentrations tended to maintain better dispersion and stability, and oxidative dissolution and precipitations of nanoparticles could occur at lower concentrations of NaHS. These would result in greater Ag diffusion into fungal mycelium, enhancing the treatment efficiency of *P. chrysosporium* (Guo et al., 2016a,b). Additionally, the undetectable levels in total Ag removal efficiency in the presence of 500 μM NaHS could be explained by the fact that AgNPs might be directly converted to the nanoparticle aggregates and/or larger-sized Ag_2S -NPs through a solid-fluid sulfidation reaction at higher NaHS concentrations, resulting in higher retention of Ag content in the media (Wirth et al., 2012; Guo et al., 2016a; Wang et al., 2015).

3.3. Removal of various heavy metals and AgNPs with NaHS pretreatment

Pb(II), Cd(II), Cu(II), Ni(II), and Zn(II) at the same initial concentrations of 100 mg/L were adopted as models of heavy metal ions. Fig. 4A shows that the capture percentages of 27% and 51% for Pb(II) and Cd(II) are observed after 24 h of exposure, whereas no removal is detected for Cu(II), Ni(II), Zn(II), and AgNP treatments when *P. chrysosporium* cells are pretreated with 100 μM NaHS. Predictably, diverse heavy metals with different adsorption sites and metal-binding energies in *P. chrysosporium* may result in different degrees of removal performance. The undetectable removal efficiency implied that *P. chrysosporium* might have weaker binding affinities to Cu(II), Ni(II), and Zn(II) than Pb(II) and Cd(II). Coupled with the observations of total Ag removal in Fig. 3, unlike heavy metals, the hindrance of Ag uptake into cells could be possibly due to NaHS-included AgNP aggregation being blocked outside the cells (Wirth et al., 2012). Moreover, effect of H_2S on Cd(II) removal was evaluated under 100-mg/L Cd(II) (Fig. 4B). Similar to Pb(II) removal, application of NaHS (0, 50, and 100 μM) enhanced removal of Cd(II) in a dose-dependent manner, with maximum efficiencies of 49%, 50%, and 55%, respectively.

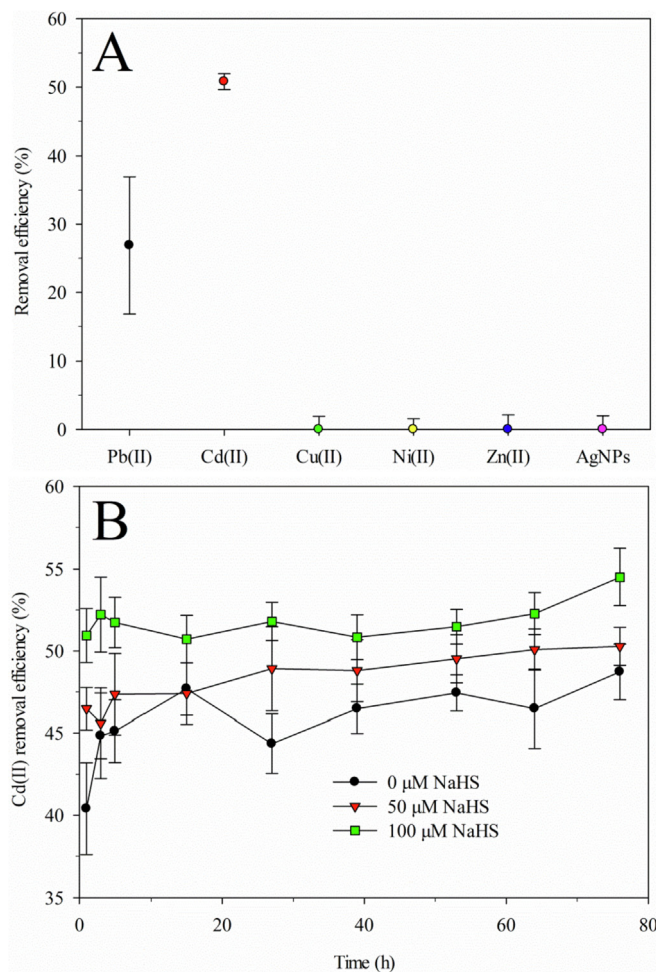


Fig. 4. (A) Removal of various heavy metals and AgNPs at initial concentrations of 100 mg/L for 24 h by *P. chrysosporium* pretreated with 100 μM NaHS; (B) time courses of 100 mg/L Cd(II) removal under 0–100 μM NaHS pretreatment.

3.4. Effects of H_2S on cell viability under heavy metal and AgNP stress

After exposure to different concentrations of Pb(II) and AgNPs for 78 h, the effects of H_2S on the tolerance of *P. chrysosporium* to Pb(II) and AgNP toxicity were investigated (Fig. 5A and B). The results showed that a concentration-dependent decrease in *P. chrysosporium* cell viability without NaHS pretreatment was observed after introduction of Pb(II) (10, 50, 100, and 200 mg/L), causing the death of approximately 25%, 40%, 55%, and 60%, respectively (Fig. 5A). A significant decrease in cell viability might be due to inhibition of cell division imparted by Pb(II) in cell wall (Ali et al., 2014). However, Pb(II)-induced cell death was dramatically reversed by NaHS pretreatment in a concentration-dependent manner. Application of 500 μM NaHS caused the most significant increase in cell viability, approximately 27%, 15%, 27%, and 39% higher viability than the untreated control, respectively. The enhancement in cell viability induced by NaHS demonstrated that H_2S exerted a strong protective effect against Pb(II) toxicity.

However, *P. chrysosporium* viability in the presence of AgNPs alone was slightly enhanced, rather than inhibited with the increasing AgNP concentrations (Fig. 5B). This could be possibly because of nanoparticle aggregation greatly reducing the direct contact/interaction between AgNPs and *P. chrysosporium* cells. Meanwhile, an obvious increase in cell viability was noticed after

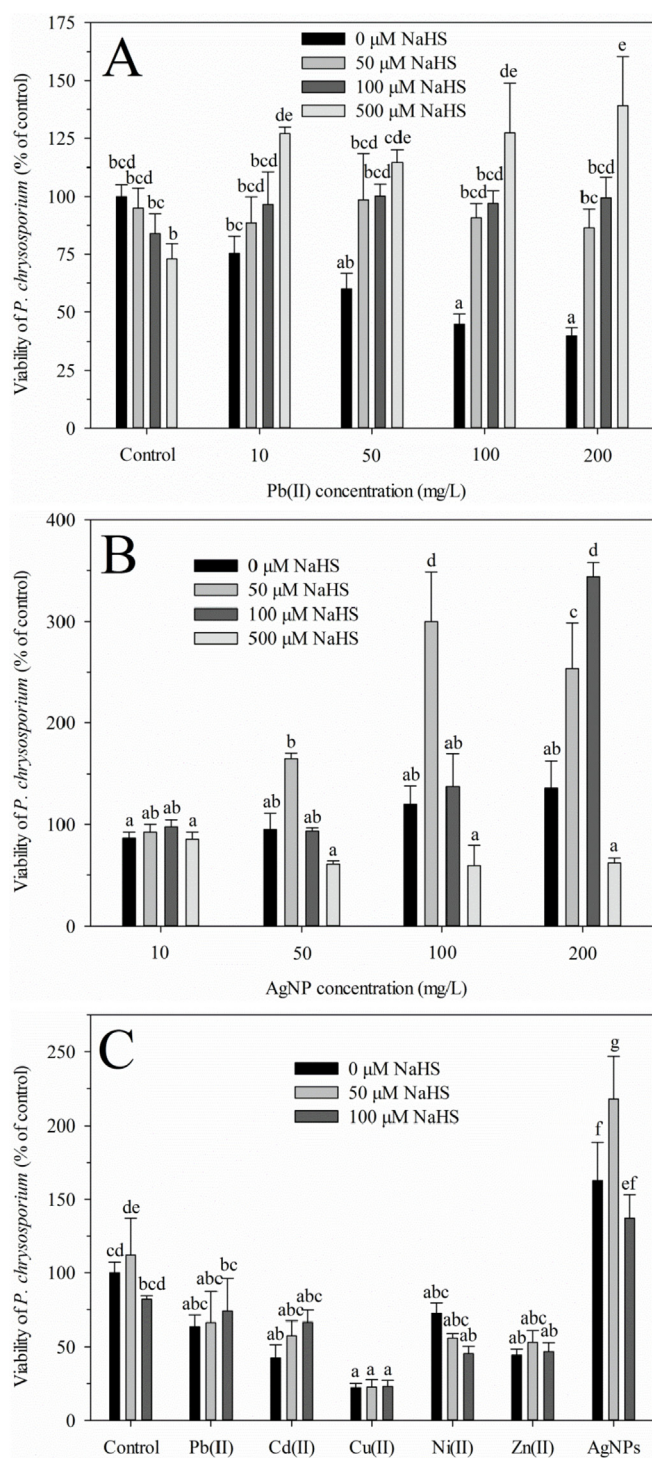


Fig. 5. Effects of different doses H₂S on cell viability after treatments with 10–200 mg/L (A) Pb(II) and (D) AgNPs for 78 h; viability of *P. chrysoisporium* pretreated with 0–100 μM NaHS after 24 h of exposure to various heavy metals and AgNPs.

pretreatment with 50 μM NaHS, except for 10-μM AgNP treatments, indicating H₂S-exerted protection against AgNP stress. With further increasing the concentrations of NaHS, however, *P. chrysoisporium* viability was remarkably depressed, resulting in substantial cell death (38%–41%) under exposure to 50–200 mg/L AgNPs following pretreatment with 500 μM NaHS. The inhibitory effects of higher concentrations of NaHS suggested that excess H₂S released might

be toxic to *P. chrysoisporium*, in agreement with the findings of previous studies (Chen et al., 2014, 2018).

Furthermore, the data regarding effects of H₂S on the viability of *P. chrysoisporium* after exposure to various heavy metals and AgNPs for 24 h are shown in Fig. 5C. In the absence of NaHS pretreatment, Pb(II), Cd(II), Cu(II), Ni(II), and Zn(II) at initial concentration of 100 mg/L led to reduction in cell viability by 36%, 57%, 78%, 28%, and 56%, respectively, as compared to the untreated control. By comparison, Cd(II), Cu(II), and Zn(II) exerted more toxic effects to *P. chrysoisporium* cells. The differential responses of cell viability to various heavy metals could be due to different sensitivities and repair abilities of *P. chrysoisporium*. After pretreatment with 50 and 100 μM NaHS, cell viability under heavy-metal stress was not significantly affected, in line with the finding reported by Shahbaz et al. (2014) who found that H₂S had little influence on Cu toxicity in *Brassica pekinensis*. By contrast, stimulation of AgNPs and NaHS on cell survival was observed when *P. chrysoisporium* cells were exposed to 100 mg/L AgNPs for 24 h. This could be attributed to the increased nanoparticle sizes and agglomeration under high-dose AgNPs and/or in the presence of NaHS (Gliga et al., 2014).

In contrast to short-term exposure (24 h), H₂S exerted the stimulatory effects on *P. chrysoisporium* survival in a concentration-dependent manner following 78 h of exposure to Pb(II) (Fig. 5A and C). The phenomena could be associated with effective removal of Pb(II) by *P. chrysoisporium* after prolonged exposure, as illustrated in Fig. 2. More enzymes were probably activated to defend against oxidative damage and to recover cell growth and replication during long-term exposure (Huang et al., 2018c).

To verify the effects of H₂S promotion on heavy metal removal and cell viability induced by NaHS, physiological analyses of *P. chrysoisporium* pretreated with and without NaHS were carried out under the stresses of various heavy metals and AgNPs.

3.5. Effects of H₂S on contents of MDA and O₂⁻

MDA content was determined to estimate the extent of lipid peroxidation under different treatments of NaHS and heavy metals (Fig. 6). Significant MDA accumulation was evoked by Pb(II), Cd(II), Cu(II), and AgNP treatments, especially in the case of Pb(II) stressed group. A higher MDA content in *P. chrysoisporium* exposed to Pb(II) demonstrated that Pb(II) could not enter into cells, but might be distributed onto the cell walls and plasma membranes (Wang et al., 2010; Xu et al., 2012b). It led to a decrease in the concentrations of unsaturated fatty acids, thus enhancing the peroxidation of membrane lipid markedly (Wang et al., 2010). Interestingly, in spite of the highest MDA level caused by Pb(II) treatment, *P. chrysoisporium* viability was not strongly inhibited. The higher tolerance of *P. chrysoisporium* to Pb(II) was likely ascribed to its highly effective antioxidant defense mechanisms. However, a significant reduction in lipid peroxidation occurred in Pb(II)-, Cd(II)-, Cu(II)-, Zn(II)-, and AgNP-stressed cells following H₂S application compared with their corresponding treatments without NaHS. The results indicated that H₂S depressed heavy metal and AgNP-induced plasma membrane damage significantly.

The production of O₂⁻ was also measured to evaluate the role of NaHS in mediating heavy metal-induced oxidative stress. Fig. 6B shows that NaHS pretreatments have no significant influence on O₂⁻ production in the control and the groups exposed to Pb(II), Ni(II), and Zn(II). However, O₂⁻ production in the NaHS-incubated *P. chrysoisporium* cells under stress of Cd(II), Cu(II), and AgNPs reduced 42%, 34%, and 46%, respectively, as compared to those without NaHS incubation, indicating the relieving effect of NaHS on O₂⁻ accumulation. Under Cu(II) stress, although NaHS-induced inhibitory effects on O₂⁻ generation occurred, the prominent production of O₂⁻ was still observed. The overproduction of free

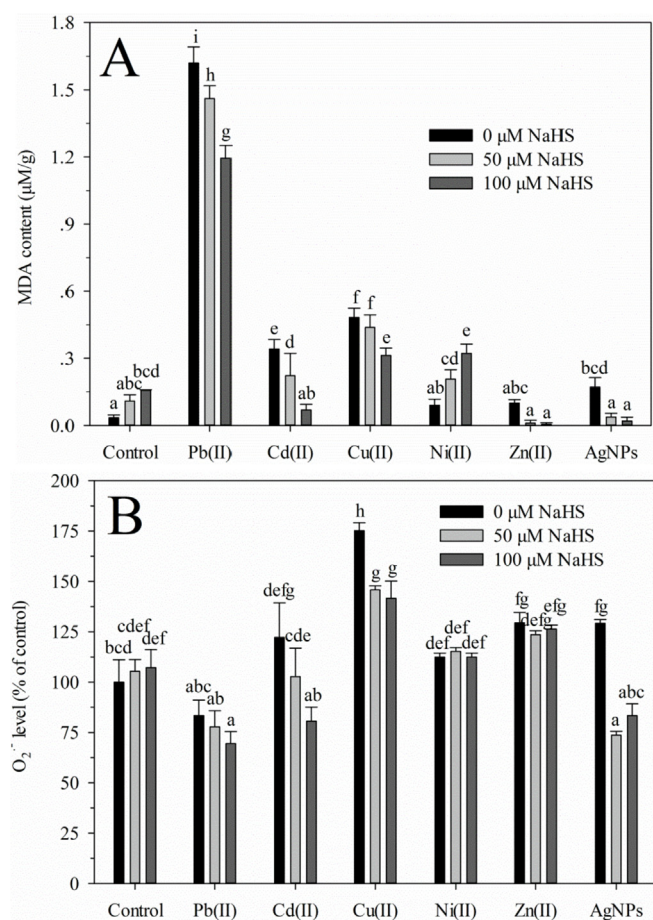


Fig. 6. Influences of H₂S on (A) MDA and (B) O₂⁻ levels in *P. chrysosporium* upon exposure to various heavy metals and AgNPs for 24 h.

radicals, not being eliminated effectively, would give rise to oxidative damage to fungal cells, resulting in a significant reduction in cell survival, as illustrated in Fig. 5C.

Taken together, H₂S seemed to be an important antioxidant signaling molecule involved in the mechanisms of tolerance against lipid peroxidation and oxidative stress induced by heavy metals and AgNPs.

3.6. Promotion of exogenous H₂S on antioxidant enzyme activities

To observe the role of H₂S on antioxidant defense system of *P. chrysosporium*, the activities of enzymes SOD and CAT under heavy-metal and AgNP stress were measured when *P. chrysosporium* was pretreated with NaHS. Higher SOD activities in the range of 136.1–214.2 U/g·Fw were obtained after introduction of Pb(II), Cd(II), Cu(II), and AgNPs, whereas, for Ni(II) and Zn(II) exposure, there was no significant difference in SOD activity relative to the untreated control (Fig. 7A). Accordingly, in comparison with Ni(II) and Zn(II), *P. chrysosporium* was more sensitive to the other metal ions and AgNPs. It has been documented that SOD activity could be stimulated by the introduction of toxic pollutants directly, such as heavy metals and AgNPs, or be increased by upregulating the expression of genes encoding SOD indirectly, in response to compensation of excess O₂⁻ generation (Zeng et al., 2012; Ma et al., 2015; Huang et al., 2018c). Importantly, SOD activities were enhanced by 102.7, 53.3, 34.3, 93.5, 61.5, 45.0, and 32.0 U/g·Fw in cells pre-incubated with NaHS under the control, Pb(II),

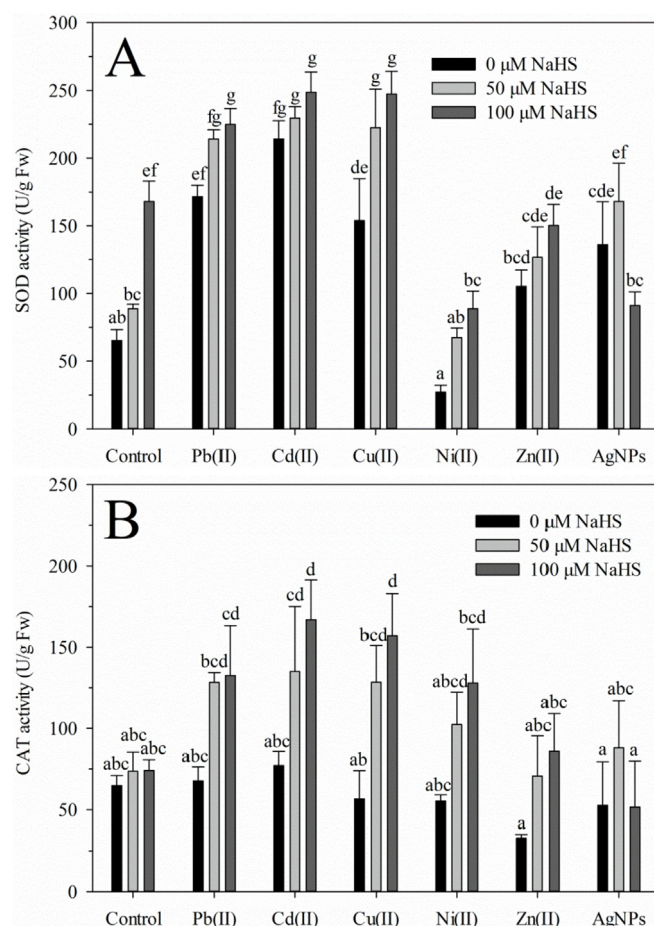


Fig. 7. (A) SOD and (B) CAT activity under different NaHS and heavy metal/AgNP treatments.

Cd(II), Cu(II), Ni(II), Zn(II), and AgNP stress, respectively, when compared to those without NaHS pre-incubation. A similar dose-dependent stimulatory effect of NaHS on CAT activity was observed when *P. chrysosporium* was subjected to the treatments with heavy metals and AgNPs (Fig. 7B). CAT activities were greatly activated in the NaHS-pretreated groups, with an increase of 35.5–100.3 U/g·Fw relative to those of the untreated groups.

Besides, it should be noted that in the absence of NaHS pretreatment, there was no significant difference in CAT activity of *P. chrysosporium* between the control and treatments with heavy metals and AgNPs. CAT activities under the control and stresses of Pb(II), Cd(II), Cu(II), Ni(II), Zn(II), and AgNPs were 64.8, 67.7, 77.2, 56.7, 55.4, 32.8, and 52.7 U/g·Fw, respectively. By contrast, changes in antioxidant enzyme activities induced by heavy metals and AgNPs had a clear difference in SOD and CAT in absence of NaHS. SOD is well-known to a key enzyme in an active oxygen scavenger system and act as the first defense line against toxic ROS for cells to adapt to biotic and abiotic stresses, catalyzing the dismutation of O₂⁻ to O₂ and H₂O₂ (Tan et al., 2015). CAT plays a vital key role in scavenging or detoxifying H₂O₂ into H₂O and O₂ (Huang et al., 2018c). Therefore, it was speculated that the lower CAT activity was probably be concerned with the higher SOD activity provoked by heavy metal and AgNP stress and that accumulation of H₂O₂ was increased due to SOD overexpression, resulting in the suppression in CAT activity (Pacini et al., 2013; Huang et al., 2018c). Another possibility for the depression of CAT was that subunits assembly and/or biosynthesis of CAT had been adversely affected by a variety

of toxic pollutants. Furthermore, the metal-enzyme complexes formed perhaps led to alterations in the structure and enzyme activity of CAT (Sun et al., 2009).

Collectively, the activities of antioxidant enzymes can be stimulated by heavy-metal and AgNP-induced ROS generation, which in turn will be scavenged by antioxidant enzymes to maintain the oxidative balance in *P. chrysosporium*, further protecting against oxidative damage to the cellular components. The levels of MDA and O_2^- were markedly lowered when the mycelia were pretreated with 50 and 100 μ M NaHS, probably because of the remarkable enhancement in activities of SOD and CAT enzymes under NaHS pretreatments. Predictably, H_2S mitigated the oxidative stress triggered by heavy metal ions and AgNPs via enhancing the expression of ROS scavenging enzymes (SOD and CAT). Similar results on NaHS-promoted tolerance to oxidative stress caused by toxicants in bacteria and fungi were also reported (Chen et al., 2014; Mironov et al., 2017; He et al., 2018a,b,c).

Furthermore, many evidences indicate that low-dose H_2S has a positive effect on growth, development, and abiotic/biotic stress resistance of animals, plants, and microorganisms (García-Mata and Lamattina, 2010; Mironov et al., 2017; Zhu et al., 2018). For example, pretreatment with NaHS (a H_2S donor) in plants can increase stress tolerance to toxic heavy metals, such as Pb, Cd, Cu, Cr, Zn, Al, and As (Chen et al., 2014; Guo et al., 2016b), and decrease the accumulation of heavy metals (Liu et al., 2016; Han et al., 2018), thereby alleviating heavy metal-induced toxicity. Conversely, in the present study, H_2S application was proven to be rewarding for improvement in removal efficacy of heavy metals Pb, Cd, and Ag. Further studies must be conducted to explore high-efficiency removal of other heavy metals and the simultaneous removal of various toxic pollutants by *P. chrysosporium* through H_2S -based technologies. Activation of *P. chrysosporium* cells could be stimulated due to the effective removal of these toxicants, and the surviving cells might induce an increase in the production of enzymes against membrane-damaging lipid peroxidation and oxidative stress. So, NaHS-induced significant increase in *P. chrysosporium* viability may be precisely due to the alleviation of oxidative stress under heavy metal and AgNP stress. Consequently, it could be concluded that H_2S plays a vital role in cell growth, antioxidant defense systems, and efficient removal of toxic pollutants in wastewater treatment.

4. Conclusions

In the present study, H_2S pretreatment improved the removal of Pb(II), Cd(II), and total Ag by *P. chrysosporium* and ameliorated heavy metal-induced growth inhibition significantly. H_2S -promoted enhancement in the activities of antioxidant enzymes was observed. Furthermore, lipid peroxidation and oxidative stress evoked by heavy metals and AgNPs were also alleviated by H_2S . Stimulation of H_2S on *P. chrysosporium* viability under heavy metal and AgNP stress could be ascribed to the upregulation of antioxidant enzymes, as well as the efficient biological removal of these toxicants. The insights in this work provide the evidence of potential applications of H_2S in bioremediation of wastewater and have great significance for advancing the mechanistic understanding of H_2S -facilitated toxicant tolerance in fungal cells.

Acknowledgements

This work was financially supported by the National Natural Science Foundation of China (51579099, 51521006, 51508186, and 51879105), the Program for Changjiang Scholars and Innovative Research Team in University (IRT-13R17).

References

- Ali, B., Song, W.J., Hu, W.Z., Luo, X.N., Gill, R.A., Wang, J., Zhou, W.J., 2014. Hydrogen sulfide alleviates lead-induced photosynthetic and ultrastructural changes in oilseed rape. *Ecotoxicol. Environ. Saf.* 102 (1), 25–33.
- Chen, A., Zeng, G., Chen, G., Zhang, C., Yan, M., Shang, C., Hu, X., Lu, L., Chen, M., Guo, Z., Zuo, Y., 2014. Hydrogen sulfide alleviates 2,4-dichlorophenol toxicity and promotes its degradation in *Phanerochaete chrysosporium*. *Chemosphere* 109, 208–212.
- Chen, Z., Yang, B., Hao, Z.K., Zhu, J., Zhang, Y., Xu, T., 2018. Exogenous hydrogen sulfide ameliorates seed germination and seedling growth of cauliflower under lead stress and its antioxidant role. *J. Plant Growth Regul.* 37, 5–15.
- Choi, Y., Kim, H.A., Kim, K.W., Lee, B.T., 2018. Comparative toxicity of silver nanoparticles and silver ions to *Escherichia coli*. *J. Environ. Sci.* 66 (4), 50–60.
- Fang, H., Liu, Z., Jin, Z., Zhang, L., Liu, D., Pei, Y., 2016. An emphasis of hydrogen sulfide-cysteine cycle on enhancing the tolerance to chromium stress in arabidopsis. *Environ. Pollut.* 213, 870–877.
- García-Mata, C., Lamattina, L., 2010. Hydrogen sulphide, a novel gasotransmitter involved in guard cell signalling. *New Phytol.* 188 (4), 977–984.
- Geng, B., Chang, L., Pan, C., Qi, Y., Zhao, J., Pang, Y., Du, J., Tang, C., 2004. Endogenous hydrogen sulfide regulation of myocardial injury induced by isoproterenol. *Biochem. Biophys. Res. Commun.* 318, 756–763.
- Gliga, A.R., Sara, S., Inger, O.W., Bengt, F., Karlsson, H.L., 2014. Size-dependent cytotoxicity of silver nanoparticles in human lung cells: the role of cellular uptake, agglomeration and Ag release. *Part. Fibre Toxicol.* 11, 11.
- Gong, J., Wang, B., Zeng, G., Yang, C., Niu, C., Niu, Q., Zhou, W., Liang, Y., 2009. Removal of cationic dyes from aqueous solution using magnetic multi-wall carbon nanotube nanocomposite as adsorbent. *J. Hazard Mater.* 164 (2–3), 1517–1522.
- Guo, Z., Chen, G., Liu, L., Zeng, G., Huang, Z., Chen, A., Hu, L., 2016b. Activity variation of *Phanerochaete chrysosporium* under nanosilver exposure by controlling of different sulfide sources. *Sci. Rep.* 6, 20813.
- Guo, Z., Chen, G., Zeng, G., Liang, J., Huang, B., Xiao, Z., Yi, F., Huang, Z., He, K., 2016a. Determination of inequable fate and toxicity of Ag nanoparticles in a *Phanerochaete chrysosporium* biofilm system through different sulfide sources. *Environ. Sci.: Nano* 3 (5), 1027–1035.
- Han, Y., Wu, M., Hao, L., Yi, H., 2018. Sulfur dioxide derivatives alleviate cadmium toxicity by enhancing antioxidant defence and reducing Cd^{2+} uptake and translocation in foxtail millet seedlings. *Ecotoxicol. Environ. Saf.* 157, 207–215.
- He, K., Chen, G., Zeng, G., Chen, A., Huang, Z., Shi, J., Huang, T., Peng, M., Hu, L., 2018a. Three-dimensional graphene supported catalysts for organic dyes degradation. *Appl. Catal., B* 228, 19–28.
- He, K., Chen, G., Zeng, G., Huang, Z., Guo, Z., Huang, T., Peng, M., Shi, J., Hu, L., 2017b. Applications of white rot fungi in bioremediation with nanoparticles and biosynthesis of metallic nanoparticles. *Appl. Microbiol. Biotechnol.* 101 (12), 1–10.
- He, K., Chen, G., Zeng, G., Peng, M., Huang, Z., Shi, J., Huang, T., 2017a. Stability, transport and ecosystem effects of graphene in water and soil environments. *Nanoscale* 9 (17), 5370–5388.
- He, K., Zeng, Z., Chen, A., Zeng, G., Xiao, R., Xu, P., Huang, Z., Shi, J., Hu, L., Chen, G., 2018b. Advancement of Ag-graphene based nanocomposites: an overview of synthesis and its applications. *Small*, 1800871, 1–13.
- He, H., Li, Y., He, L.F., 2018c. The central role of hydrogen sulfide in plant responses to toxic metal stress. *Ecotoxicol. Environ. Saf.* 157, 403–408.
- Houda, Z., Bejaoui, Z., Albouchi, A., Gupta, D.K., Corpas, F.J., 2016. Comparative study of plant growth of two poplar tree species irrigated with treated wastewater, with particular reference to accumulation of heavy metals (Cd, Pb, As, and Ni). *Environ. Monit. Assess.* 188 (2), 99.
- Huang, Z., Chen, G., Zeng, G., Chen, A., Zuo, Y., Guo, Z., Tan, Q., Song, Z., Niu, Q., 2015. Polyvinyl alcohol-immobilized *Phanerochaete chrysosporium* and its application in the bioremediation of composite-polluted wastewater. *J. Hazard Mater.* 289, 174–183.
- Huang, Z., Chen, G., Zeng, G., Guo, Z., He, K., Hu, L., Wu, J., Zhang, L., Zhu, Y., Song, Z., 2017. Toxicity mechanisms and synergies of silver nanoparticles in 2,4-dichlorophenol degradation by *Phanerochaete chrysosporium*. *J. Hazard Mater.* 321, 37–46.
- Huang, Z., He, K., Song, Z., Zeng, G., Chen, A., Yuan, L., Li, H., Hu, L., Guo, Z., Chen, G., 2018c. Antioxidative response of *Phanerochaete chrysosporium* against silver nanoparticle-induced toxicity and its potential mechanism. *Chemosphere* 211, 573–583.
- Huang, Z., Xu, P., Chen, G., Zeng, G., Chen, A., Song, Z., He, K., Yuan, L., Li, H., Hu, L., 2018a. Silver ion-enhanced particle-specific cytotoxicity of silver nanoparticles and effect on the production of extracellular secretions of *Phanerochaete chrysosporium*. *Chemosphere* 196, 575–584.
- Huang, Z., Zeng, Z., Chen, A., Zeng, G., Xiao, R., Xu, P., He, K., Song, Z., Hu, L., Peng, M., Huang, T., Chen, G., 2018b. Differential behaviors of silver nanoparticles and silver ions towards cysteine: bioremediation and toxicity to *Phanerochaete chrysosporium*. *Chemosphere* 203, 199–208.
- Leng, L., Huang, H., Li, H., Li, J., Zhou, W., 2019. Biochar stability assessment methods: a review. *Sci. Total Environ.* 647, 210–222.
- Liu, X., Chen, J., Wang, G.H., Wang, W.H., Shen, Z.J., Luo, M.R., Gao, G.F., Simon, M., Ghoto, K., Zheng, H.L., 2016. Hydrogen sulfide alleviates zinc toxicity by reducing zinc uptake and regulating genes expression of antioxidative enzymes and metallothioneins in roots of the cadmium/zinc hyperaccumulator *Solanum*

- nigrum* L. Plant Soil 400 (1–2), 177–192.
- Ma, C., Chhikara, S., Minocha, R., Long, S., Musante, C., White, J.C., Xing, B., Dhankher, O.P., 2015. Reduced silver nanoparticle phytotoxicity in *Crambe abysinnica* with enhanced glutathione production by overexpressing bacterial γ -glutamylcysteine synthase. Environ. Sci. Technol. 49, 10117–10126.
- Macomber, L., Hausinger, R.P., 2011. Mechanisms of nickel toxicity in microorganisms. Metallomics 3 (11), 1153–1162.
- McGillcuddy, E., Murray, I., Kavanagh, S., Morrison, L., Fogarty, A., Cormican, M., Dockery, P., Prendergast, M., Rowan, N., Morris, D., 2017. Silver nanoparticles in the environment: sources, detection and ecotoxicology. Sci. Total Environ. 575, 231–246.
- Mironov, A., Seregina, T., Nagornykh, M., Luhachack, L.G., Korolkova, N., Lopes, L.E., Kotova, V., Zavigelsky, G., Shakulov, R., Shatalin, A., Nudler, E., 2017. Mechanism of H₂S-mediated protection against oxidative stress in *Escherichia coli*. Proc. Natl. Acad. Sci. U.S.A. 114 (23), 6022–6027.
- Mir-Tutusaus, J.A., Bacchar, R., Caminal, G., Sarra, M., 2018. Can white-rot fungi be a real wastewater treatment alternative for organic micropollutants removal? A review. Water Res. 138, 137–151.
- Mitsuhashi, H., Yamashita, S., Ikeuchi, H., Kuroiwa, T., Kaneko, Y., Kiromura, K., Ueki, K., Nojima, Y., 2006. Oxidative stress-dependent conversion of hydrogen sulfide to sulfite by activated neurophils. Shock 24, 529.
- Pacini, N., Elia, A.C., Abete, M.C., Dorr, P., Brizio, A.J.M., Gasco, L., Righetti, M., Prearo, M., 2013. Antioxidant response versus selenium accumulation in the liver and kidney of the Siberian sturgeon (*Acipenser baeri*). Chemosphere 93 (10), 2405–2412.
- Qin, L., Zeng, G., Lai, C., Huang, D., Xu, P., Zhang, C., Cheng, M., Liu, X., Liu, S., Li, B., Yi, H., 2018. "Gold rush" in modern science: fabrication strategies and typical advanced applications of gold nanoparticles in sensing. Coord. Chem. Rev. 359, 1–31.
- Ren, X., Zeng, G., Tang, L., Wang, J., Wan, J., Feng, H., Song, B., Huang, C., Tang, X., 2018a. Effect of exogenous carbonaceous materials on the bioavailability of organic pollutants and their ecological risks. Soil Biol. Biochem. 116, 70–81.
- Ren, X., Zeng, G., Tang, L., Wang, J., Wan, J., Liu, Y., Yu, J., Yi, H., Ye, S., Deng, R., 2018b. Sorption, transport and biodegradation - an insight into bioavailability of persistent organic pollutants in soil. Sci. Total Environ. 610–611, 1154–1163.
- Shahbaz, M., Stuiver, C.E.E., Posthumus, F.S., Parmar, S., Hawkesford, M.J., De Kok, L.J., 2014. Copper toxicity in Chinese cabbage is not influenced by plant sulphur status, but affects sulphur metabolism-related gene expression and the suggested regulatory metabolites. Plant Biol. 16, 68–78.
- Sun, S.Q., He, M., Cao, T., Zhang, Y.C., Han, W., 2009. Response mechanisms of antioxidants in bryophyte (*Hypnum plumaeforme*) under the stress of single or combined Pb and/or Ni. Environ. Monit. Assess. 149 (1), 291–302.
- Tan, Q., Chen, G., Zeng, G., Chen, A., Guan, S., Li, Z., Zuo, Y., Huang, Z., Guo, Z., 2015. Physiological fluxes and antioxidative enzymes activities of immobilized *Phanerochaete chrysosporium* loaded with TiO₂ nanoparticles after exposure to toxic pollutants in solution. Chemosphere 128, 21–27.
- Tang, X., Zeng, G., Fan, C., Zhou, M., Tang, L., Zhu, J., Wan, J., Huang, D., Chen, M., Xu, P., Zhang, C., Xiong, W., 2018. Chromosomal expression of CadR on *Pseudomonas aeruginosa* for the removal of Cd(II) from aqueous solutions. Sci. Total Environ. 636, 1355–1361.
- Wang, H., Yuan, X., Wu, Y., Chen, X., Leng, L., Zeng, G., 2015. Photodeposition of metal sulfides on titanium metal-organic frameworks for excellent visible-light-driven photocatalytic Cr(VI) reduction. RSC Adv. 5, 32531–32535.
- Wang, H., Yuan, X., Wu, Y., Huang, H., Zeng, G., Liu, Y., Wang, X., Lin, N., Qi, Y., 2013. Adsorption characteristics and behaviors of graphene oxide for Zn(II) removal from aqueous solution. Appl. Surf. Sci. 279, 432–440.
- Wang, L., Zhou, Q., Zhao, B., Huang, X., 2010. Toxic effect of heavy metal terbium ion on cell membrane in horseradish. Chemosphere 80 (1), 28–34.
- Wang, Y., Zhu, Y., Hu, Y., Zeng, G., Zhang, Y., Zhang, C., Feng, C., 2018. How to construct DNA hydrogels for environmental applications: advanced water treatment and environmental analysis. Small 14 (1703355), 1–19.
- Wirth, S.M., Lowry, G.V., Tilton, R.D., 2012. Natural organic matter alters biofilm tolerance to silver nanoparticles and dissolved silver. Environ. Sci. Technol. 46, 12687–12696.
- Wu, F., Harper, B.J., Harper, S.L., 2017. Differential dissolution and toxicity of surface functionalized silver nanoparticles in small-scale microcosms: impacts of community complexity. Environ. Sci.: Nano 4, 359–372.
- Xiong, W., Zeng, Z., Li, X., Zeng, G., Xiao, R., Yang, Z., Zhou, Y., Zhang, C., Cheng, M., Hu, L., Zhou, C., Qin, L., Xu, R., Zhang, Y., 2018. Multi-walled carbon nanotube/amino-functionalized MIL-53(Fe) composites: remarkable adsorptive removal of antibiotics from aqueous solutions. Chemosphere 210, 1061–1069.
- Xu, P., Zeng, G.M., Huang, D.L., Feng, C.L., Hu, S., Zhao, M.H., Lai, C., Wei, Z., Huang, C., Xie, G.X., Liu, Z.F., 2012a. Use of iron oxide nanomaterials in wastewater treatment: a review. Sci. Total Environ. 424, 1–10.
- Xu, P., Zeng, G.M., Huang, D.L., Lai, C., Zhao, M.H., Wei, Z., Li, N.J., Huang, C., Xie, G.X., 2012b. Adsorption of Pb(II) by iron oxide nanoparticles immobilized *Phanerochaete chrysosporium*: equilibrium, kinetic, thermodynamic and mechanisms analysis. Chem. Eng. J. 203, 423–431.
- Yang, Y., Zeng, Z., Zhang, C., Huang, D., Zeng, G., Xiao, R., Lai, C., Zhou, C., Guo, H., Xue, W., Cheng, M., Wang, W., Wang, J., 2018a. Construction of iodine vacancy-rich BiOI/Ag@AgI Z-scheme heterojunction photocatalysts for visible-light-driven tetracycline degradation: transformation pathways and mechanism insight. Chem. Eng. J. 349, 808–821.
- Yang, Y., Zhang, C., Lai, C., Zeng, G., Huang, D., Cheng, M., Wang, J., Chen, F., Zhou, C., Xiong, W., 2018b. BiOX (X = Cl, Br, I) photocatalytic nanomaterials: applications for fuels and environmental management. Adv. Colloid Interface Sci. 254, 77–93.
- Ye, S., Zeng, G., Wu, H., Zhang, C., Dai, J., Liang, J., Yu, J., Ren, X., Yi, H., Cheng, M., Zhang, C., 2017a. Biological technologies for the remediation of co-contaminated soil. Crit. Rev. Biotechnol. 37 (8), 1062–1076.
- Ye, S., Zeng, G., Wu, H., Zhang, C., Liang, J., Dai, J., Liu, Z., Xiong, W., Wan, J., Xu, P., Cheng, M., 2017b. Co-occurrence and interactions of pollutants, and their impacts on soil remediation—a review. Crit. Rev. Environ. Sci. Technol. 47 (16), 1528–1553.
- Yi, H., Huang, D., Qin, L., Zeng, G., Lai, C., Cheng, M., Ye, S., Song, B., Ren, X., Guo, X., 2018. Selective prepared carbon nanomaterials for advanced photocatalytic application in environmental pollutant treatment and hydrogen production. Appl. Catal., B 239, 408–424.
- Yuan, Y., Zheng, J., Zhao, T., Tang, X., Hu, N., 2017. Hydrogen sulfide alleviates uranium-induced acute hepatotoxicity in rats: role of antioxidant and anti-apoptotic signaling. Environ. Toxicol. 32 (2), 581–593.
- Zeng, G.M., Chen, A.W., Chen, G.Q., Hu, X.J., Guan, S., Shang, C., Lu, L.H., Zou, Z.J., 2012. Responses of *Phanerochaete chrysosporium* to toxic pollutants: physiological flux, oxidative stress, and detoxification. Environ. Sci. Technol. 46, 7818–7825.
- Zhang, C., Wang, W., Duan, A., Zeng, G., Huang, D., Lai, C., Tan, X., Cheng, M., Wang, R., Zhou, C., Xiong, W., Yang, Y., 2019. Adsorption behavior of engineered carbons and carbon nanomaterials for metal endocrine disruptors: experiments and theoretical calculation. Chemosphere 222, 184–194.
- Zhang, L., Zhang, J., Zeng, G., Dong, H., Chen, Y., Huang, C., Zhu, Y., Xu, R., Cheng, Y., Hou, K., Cao, W., Fang, W., 2018. Multivariate relationships between microbial communities and environmental variables during co-composting of sewage sludge and agricultural waste in the presence of PVP-AgNPs. Bioresour. Technol. 261, 10–18.
- Zhou, C., Lai, C., Zhang, C., Zeng, G., Huang, D., Cheng, M., Hu, L., Xiong, W., Chen, M., Wang, J., Yang, Y., Jiang, L., 2018. Semiconductor/boron nitride composites: synthesis, properties, and photocatalysis applications. Appl. Catal., B 238, 6–18.
- Zhu, C.Q., Zhang, J.H., Sun, L.M., Zhu, L.F., Abliz, B., Hu, W.J., Zhong, C., Bai, Z.G., Sajid, H., Cao, X.C., Jin, Q.Y., 2018. Hydrogen sulfide alleviates aluminum toxicity via decreasing apoplast and symplast Al contents in rice. Front. Plant Sci. 9, 294.